SCIENTIFIC REPORTS
nature research

OPEN

miR302a and 122 are deregulated in small extracellular vesicles from ARPE-19 cells cultured with H_2O_2

Maria Oltra[1,2,3], Lorena Vidal-Gil[1,2,3], Rosa Maisto[4], Sara S. Oltra[5], Francisco Javier Romero[6], Javier Sancho-Pelluz[2,3*] & Jorge Miguel Barcia[2,3]

Age related macular degeneration (AMD) is a common retina-related disease leading to blindness. Little is known on the origin of the disease, but it is well documented that oxidative stress generated in the retinal pigment epithelium and choroid neovascularization are closely involved. The study of circulating miRNAs is opening new possibilities in terms of diagnosis and therapeutics. miRNAs can travel associated to lipoproteins or inside small Extracellular Vesicles (sEVs). A number of reports indicate a significant deregulation of circulating miRNAs in AMD and experimental approaches, but it is unclear whether sEVs present a significant miRNA cargo. The present work studies miRNA expression changes in sEVs released from ARPE-19 cells under oxidative conditions (i.e. hydrogen peroxide, H_2O_2). H_2O_2 increased sEVs release from ARPE-19 cells. Moreover, 218 miRNAs could be detected in control and H_2O_2 induced-sEVs. Interestingly, only two of them (hsa-miR-302a and hsa-miR-122) were significantly under-expressed in H_2O_2-induced sEVs. Results herein suggest that the down regulation of miRNAs 302a and 122 might be related with previous studies showing sEVs-induced neovascularization after oxidative challenge in ARPE-19 cells.

microRNA (miRNA) are small non-coding RNA sequences (21-25 nucleotides) able to regulate the expression of one or more mRNAs[1,2]. miRNAs regulate protein translation by targeting their complementary mRNAs and by repressing translation or degrading a target mRNA. Nowadays, miRNA research has been rocketed from 214 publications in 2014 to 11,610 in 2018 (source: Pubmed). Many clinical fields are now focused on the study of miRNA for diagnosis or treatment purposes[3,4]. Moreover, miRNAs play an important role in different cellular processes such as angiogenesis[5,6], oxidative stress[7], and immune responses[8].

Most of the cells can release extracellular vesicles (EVs), which may interact with both neighbouring or distant target cells[9,10]. EVs typically include genetic material and proteins, making these vesicles key in cell to cell communication[11]. Among these EVs, are the small EVs (sEVs; <100 nm diameter)[12], which were observed to carry miRNAs[13]. Cargo of sEVs depends on the cellular origin and the homeostatic state[14].

Recent studies analysed miRNA expression in biological samples from patients with age related macular degeneration (AMD), in order to identify those miRNAs related to the pathophysiology and progression of the disease. Among these, miR-9, miR-23a, miR-27a, miR-34a, miR-146a, miR-155 have been proposed as potential candidates[15–19]. The "wet" form of AMD is characterized by neovascularization[20]. The retinal pigment epithelium (RPE) plays a pivotal role between the photoreceptor cell layer and the choroid, the vascular network surrounding the eye. This interaction is critical for retinal homeostasis[21]. Ren and collaborators analysed circulating miRNAs from AMD patients and proposed miR-27a-3p, miR-29b-3p, and miR-195-5p as candidate biomarkers for AMD diagnosis[19].

One of the most challenging issues in ophthalmological sciences is to identify early markers for AMD in order to prevent its clinical evolution. To date AMD treatments are limited to diminish the evolution of the disease as anti-VEGF drugs (eg. Bevacizumab)[22]. The present work studies the oxidative-induced response in RPE cells, in order to find potential miRNAs related to neovascularization within sEVs.

[1]Escuela de Doctorado Universidad Católica de Valencia San Vicente Mártir, Valencia, Spain. [2]Neurobiología y Neurofisiología, Facultad de Medicina y Ciencias de la Salud, Universidad Católica de Valencia San Vicente Mártir, Valencia, Spain. [3]Centro de Investigación Traslacional San Alberto Magno, Universidad Católica de Valencia San Vicente Mártir, Valencia, Spain. [4]Università degli studi della Campania Luigi Vanvitelli, Naples, Italy. [5]INCLIVA Biomedical Research Institute, Hospital Clínico Universitario Valencia, University of Valencia, Valencia, Spain. [6]Hospital General de Requena, Valencia, Spain. *email: fj.sancho@ucv.es

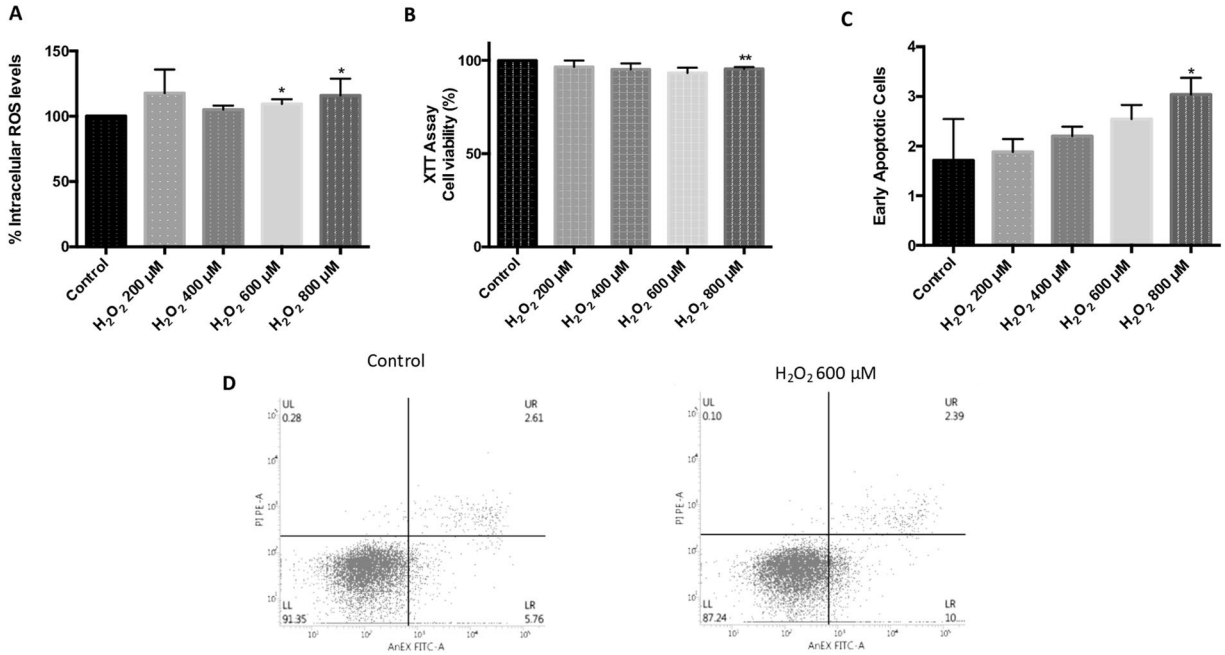

Figure 1. Effect of oxidative stress in ARPE-19 cells. Superoxide anions were measured by DHE after 24 h of H_2O_2 treatment. (**A**) XTT cell viability as percentage to control. (**B**) Early apoptotic cells measured using AnnexinV-IP. (**C**) Flow cytometry histograms: alive cells (annexin V^-, PI^-), early apoptosis (annexin V^+, PI^-) and necrotic cells (annexin V^+, IP^+). (**D**) Values are expressed as mean ± SEM (n = 3). Statistically significant differences were set at *$p < 0.05$ and **$p < 0.01$.

Results

H_2O_2-induced oxidative stress in ARPE-19 cells. ARPE-19 cells exposed for 24 h to H_2O_2 significantly increased intracellular reactive oxygen species (ROS) levels when using a concentration of 600 µM (106 ± 1.69) and 800 µM (103.1 ± 0.9892), compared to control (100 ± 0). Nevertheless, 400 µM H_2O_2, or lower, did not increase ROS levels compared to control (Fig. 1A). In order to assess whether H_2O_2-induced ROS affected ARPE-19 cell viability, a XTT assay was performed. Cell viability was significantly decreased when using 800 µM H_2O_2 (95.45 ± 0.9999) but not with lower concentrations (Fig. 1B). Moreover, 800 µM H_2O_2 concentration also increased early apoptosis (3.038 ± 0.1689) with respect to control (1.713 ± 0.4796) (Fig. 1C,D).

H_2O_2 increased sEVs release in ARPE-19. Matching previous results on cell viability (see Fig. 1), 600 µM H_2O_2 was used to stress ARPE-19 cells without killing them (sub-lethal concentration). After 24 h of 600 µM H_2O_2 exposure, ARPE-19 cells significantly increased the number of EVs released to the medium (Fig. 2). More precisely, a 40% increase in the release of EVs was observed after 600 µM H_2O_2 exposure, compared to controls. Number and size of EVs were studied using a nanoparticle tracking system (NanoSight) (Fig. 2A). Besides, EVs were observed using transmission electron microscopy (TEM), which showed that, according to size and morphology, most of the EVs observed can be classified as sEVs (Fig. 2B,C).

miRNA Expression in ARPE-19 cells and sEVs. In the present study, 384 miRNAs were analysed, and two different miRNA clusters could be set after hierarchical clustering (Fig. 3). The same proceeding was performed with the extracellular medium to collect sEVs and miRNAs providing also two clusters (Fig. 4).

miRNA Expression in ARPE-19 cells (Cell miRNA). As shown in Fig. 3, there is a significant miRNA repression after H_2O_2 treatment when compared with control ARPE-19 cells. As a result, 306 out of 384 Cell miRNAs were detected by the array. From those, 59 Cell miRNAs were significantly expressed in ARPE-19 cells ($p < 0.05$) (Table 1). Moreover, seven out of 59 Cell miRNAs were significantly under-expressed in H_2O_2-treated cells (fold change, FC > 1) than in control conditions. Different detected miRNAs are shown in Fig. 5A,C. It is noteworthy to underline that hsa-miR-205 and hsa-miR-302c presented a dramatic decrease in treated cells when compared to others (FC > 2).

miRNA Expression in ARPE-19 sEVs (sEV miRNA). As above-mentioned, ARPE-19 cells released a significantly higher number of sEVs after 600 µM H_2O_2 exposure than control cells. In contrast, these H_2O_2 induced sEVs showed a significant lower miRNA expression compared to control. More concretely, 218 out of 384 sEV miRNAs were detected by the array. However, only 2 out of 218 sEV miRNAs were significantly lower in sEVs released from treated cells ($p < 0.05$) hsa-miR-302a (FC = 1.159) and hsa-miR-122 (FC = 1.576) than in control sEVs (Fig. 5B,D).

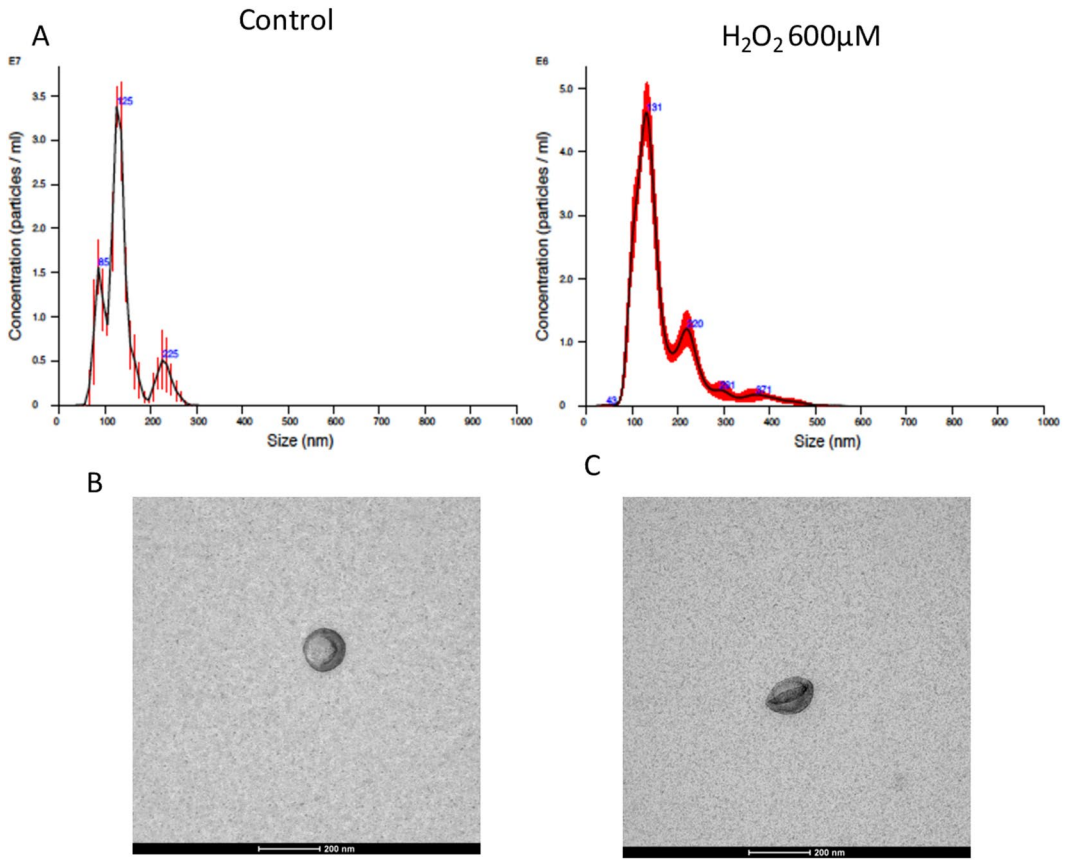

Figure 2. Characterization of sEVs released by ARPE-19 cells. Size-distribution analysis and sEVs number were performed by Nanoparticle Tracking Analysis. (**A**) EVs released by ARPE-19 cells control (**B**) and ARPE-19 cells treated by 600 µM H_2O_2 (**C**) were detected by electron microscopy.

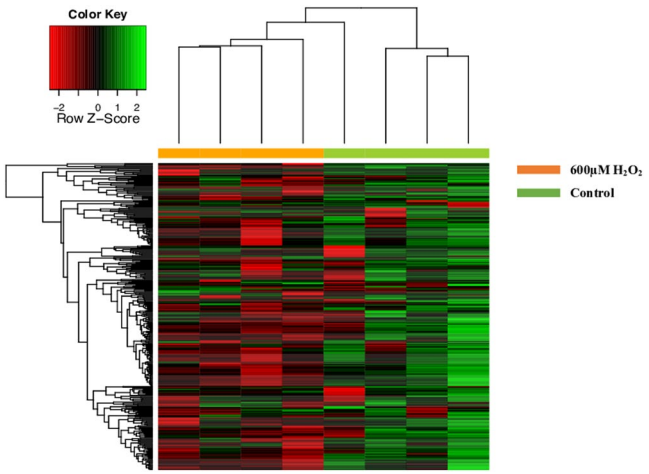

Figure 3. Heatmap of miRNA expression profile from array assay of ARPE-19 cells. After 24 h of 600 µM H_2O_2, the miRNA expression profile was analyzed, using an array for microRNA. Hierarchical unsupervised clustering was performed with the expressed miRNAs in ARPE-19 cells. Each column represents an individual cell sample. Orange columns are ARPE-19 cells treat with 600 µM H_2O_2 and green columns ARPE-19 cell controls. Control sample (n = 4) and 600 µM H_2O_2 sample (n = 4). The overexpressed miRNAs are shown in green and under-expressed miRNAs in red. Expression values are calculated with respect to the reference genes of the array assay.

Microarray validation. Among the miRNAs differently expressed in ARPE-19 cells, seven out of 59 presented a significant fold-change. In order to validate this finding, qRT-PCR was performed by using independent RNA samples. We selected three out of seven significant miRNAs (those with the highest differences observed):

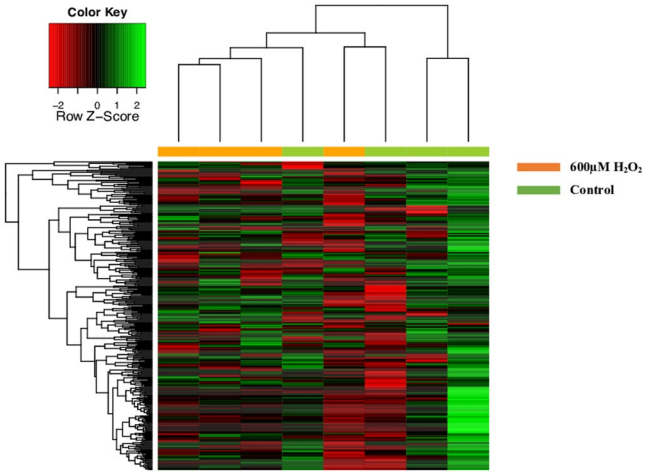

Figure 4. Heatmap of miRNA expression profile from array assay of the sEVs released by ARPE-19 cells. After 24 h of 600 μM H_2O_2, the miRNA expression profile of sEVs was analyzed, using an array of microRNA. Hierarchical unsupervised clustering was performed with the expressed miRNAs in ARPE-19-released sEVs. Each column represents an individual cell sample. Orange columns are sEVs released by ARPE-19 cells treat with 600 μM H_2O_2 and green columns are sEVs released by ARPE-19 control cells. Control sample (n = 4) and 600 μM H_2O_2 sample (n = 4). Overexpressed miRNAs (green) and under-expressed miRNAs (red). The expression values are calculated with respect to the reference genes of the array.

miRNA	FC	P_value	miRNA	FC	P_value
hsa-miR-139-3p	0,71	0,00065	**hsa-miR-371-5p**	0,95	0,02665
hsa-miR-192	0,74	0,00129	**hsa-miR-92a**	0,70	0,02672
hsa-miR-22	0,73	0,00646	**hsa-miR-361-5p**	0,79	0,02674
hsa-miR-15b	0,73	0,00657	**hsa-miR-521**	1,35	0,02850
hsa-let-7c	0,82	0,00661	**hsa-miR-30c**	0,78	0,02935
hsa-let-7b	0,77	0,00670	**hsa-miR-335**	0,85	0,03051
hsa-miR-221	0,66	0,00723	**hsa-miR-28-5p**	0,94	0,03170
hsa-miR-323-5p	0,79	0,01131	**hsa-let-7g**	0,84	0,03204
hsa-miR-15a	0,67	0,01139	**hsa-miR-29c**	0,82	0,03218
hsa-miR-18b	0,70	0,01164	**hsa-miR-488**	0,98	0,03271
hsa-miR-151-3p	0,78	0,01193	**hsa-miR-532-3p**	0,86	0,03316
hsa-miR-183	0,80	0,01214	**hsa-miR-338-5p**	1,11	0,03332
hsa-miR-518b	0,76	0,01364	**hsa-miR-125a-5p**	0,82	0,03352
hsa-miR-10a	0,78	0,01407	**hsa-miR-499-3p**	0,72	0,03376
hsa-miR-23a	0,79	0,01456	**hsa-miR-29a**	0,72	0,03509
hsa-miR-151-5p	0,85	0,01492	**hsa-miR-20b**	0,81	0,03536
hsa-miR-224	0,78	0,01537	**hsa-miR-148a**	0,90	0,03727
hsa-miR-186	0,52	0,01561	**hsa-miR-548b-5p**	1,91	0,03849
hsa-let-7f	0,86	0,01619	**hsa-miR-218**	1,00	0,04031
hsa-miR-27a	0,80	0,01739	**hsa-miR-505**	0,65	0,04090
hsa-miR-148b	0,66	0,01813	**hsa-miR-205**	2,29	0,04350
hsa-miR-25	0,83	0,01956	**hsa-miR-17**	0,78	0,04392
hsa-miR-98	1,00	0,01966	**hsa-miR-324-5p**	0,73	0,04490
hsa-miR-106a	0,71	0,02016	**hsa-miR-320c**	0,82	0,04523
hsa-let-7a	1,06	0,02102	**hsa-miR-99a**	0,84	0,04595
hsa-miR-300	0,89	0,02126	**hsa-miR-302c**	2,55	0,04598
hsa-miR-18a	0,70	0,02210	**hsa-miR-30b**	0,85	0,04622
hsa-miR-515-3p	0,89	0,02262	**hsa-miR-28-3p**	0,83	0,04717
hsa-miR-27b	0,78	0,02454	**hsa-miR-99**	0,77	0,04962
hsa-miR-518d-3p	1,06	0,02537			

Table 1. miRNAs significantly regulated in ARPE-19 cells under oxidative stress. The miRNAs are ranged according to the P-value.

A

miRNA name	FC	P_value	Control mean	Treated mean
Let-7a	1,056	0,021	1,153	0,097
Hsa-miR-518d-3p	1,056	0,025	1,202	0,146
Hsa-miR-521	1,348	0,028	1,459	0,315
Hsa-miR-338-5p	1,108	0,033	1,258	0,149
Hsa-miR-548b-5p	1,908	0,038	2,08	0,176
Hsa-miR-205	2,287	0,043	2,618	0,331
Hsa-miR-302c	2,55	0,046	2,697	0,145

B

miRNA name	FC	P_value	Control mean	Treated mean
Hsa-miR-302a	1,159	0,020	1,251	0,092
Hsa-miR-122	1,576	0,049	1,581	0,005

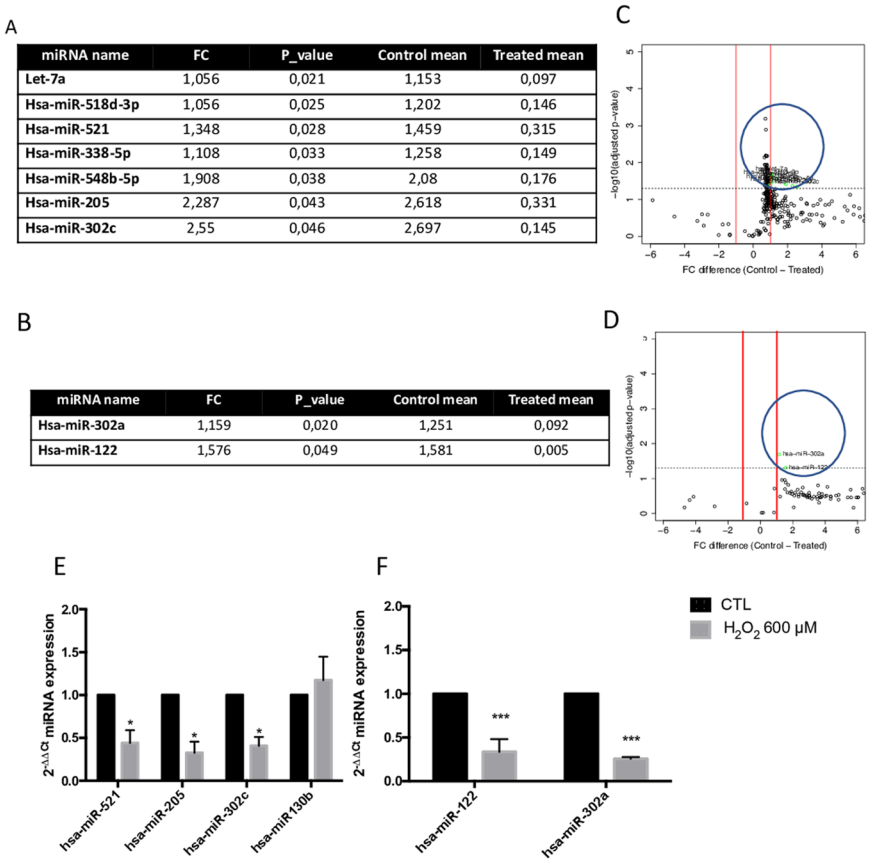

Figure 5. miRNAs significantly regulated in ARPE-19 cells. Cell miRNAs (**A**) and sEV miRNA (**B**) up-regulated in ARPE-19 cells with fold change (FC) > 1. Volcano plot of miRNA expression profile. The X axis represent the miRNA expression level and the Y axis represents p-value (T-student Test). The red lines indicate FC ± 1 P < 0.05 (**C**,**D**). Relative expression of the selected Cell miRNAs (**E**) and sEV miRNAs (**F**) with FC > 1 (control vs 600 µM H_2O_2). miRNA expression was quantified by qRT-PCR and calculate using the $2^{-\Delta\Delta Ct}$. The p-value was calculated by Two-way ANOVA. Results are expressed as mean ± SEM of n = 3–4. *p-value < 0.05 vs Control and ***p-value < 0.001.

hsa-miR-205-5p, hsa-miR-521, and hsa-miR-302c; plus a miRNA that was unchanged: hsa-miR-130b, as a control. The outcome confirmed the results obtained, hsa-miR-205-5p, hsa-miR-521 and hsa-miR-302c were down-regulated by 600 µM H_2O_2 compared to control (Fig. 5E).

The same procedure, qRT-PCR, was performed using the two sEV miRNAs which expression had changed: hsa-miR-302a and hsa-miR-122. As expected, miRNAs were under-expressed in sEVs released from ARPE-19 cells treated with 600 µM H_2O_2 (Fig. 5F).

Pathway analysis and prediction of miRNA targets regulated by oxidative stress. Subsequently, the role of the under-expressed miRNAs in treated ARPE-19 cells and in sEVs from treated cells (seven in cells and two in sEVs), was analysed. For that reason, two independent ¨*in silico*¨ analysis were performed in order to determine potential biological processes related to oxidative stress induction. The analysis of the KEGG pathway, regulated by Let-7a, miR-518d-3p, miR-521, miR-338-5p, miR-548b-5p, miR-205, and miR-302c, shows a large number of pathways involving these miRNAs. Among them, cell cycle, adherent junction, p53 signalling pathway, and HIF-1 signalling pathway are the most relevant (Fig. 6A). Both sEV miRNAs, miR-302a and miR-122, are involved in different pathways, such as TGF-beta signalling pathway, FoxO signalling pathway, and cell cycle (Fig. 7A).

Potential targets of miRNAs. In order to identify biological functions of the validated miRNAs and to select their putative targets, two programs were handled: DIANA TOOLS mirPath and Target Scan Human. The outcome on sEV miRNA and Cell miRNA related pathways are not completely equivalent. Most of the significantly involved KEGG are related to cancer or cell cycle pathways (Figs. 6B and 7B).

Discussion

The study of circulating miRNAs on AMD has been addressed to find biological markers which might help implementing an early diagnosis for the disease, or to find new therapeutic strategies[18]. Although neovascular processes and oxidative stress are well known characters involved on AMD, the origin of the disease is far from being completely understood. Several studies were focused in identifying neovascularization-related miRNAs or oxidative

A

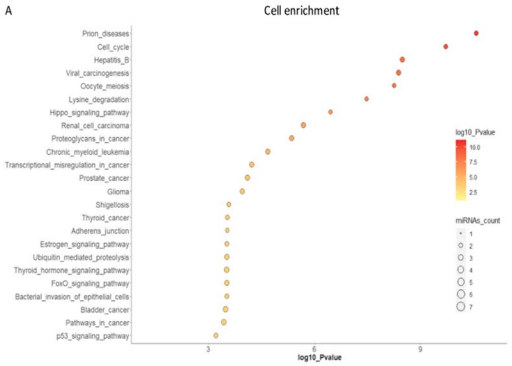

B

KEGG pathway	P_value	Number of miRNAs	Putative target genes
Nucleotide excision repair	0,00078	2	PCNA GTF2H1 POLD3 MNAT1 DDB1 POLE4 ERCC4 RBX1 RPA2
Hippo signaling pathway	0,00078	2	FZD5 YAP1 BTRC CCND2 AREG FZD6 SNAI2 MOB1B MPP5 DLG4 CCND1 MOB1A LATS TGFBR2 CTGF PPP1CB SCRIB
Transcriptional misregulation in cancer	0,00078	3	TMPRSS2 NFKB1 ELK4 RUNX1 AFF1 CCND2 RUNX2 TP53 KLF3 BMP2K EWSR1 JUP TGFBR2
Viral carcinogenesis	0,00078	3	NFKB2 NRAS IRF9 GTF2H1 CCND2 CDK1 CDK6 TP53 HNRNPK CREB1 CCND1 SKP2 DDB1 GTF2A2 SRC CDC20 HRAS SNW1 SCRIB
Glioma	0,00078	3	E2F1 NRAS CALM1 CDK6 TP53 CCND1 AKT1 HRAS MAP2K1 PTEN
Thyroid cancer	0,00078	3	NRAS TP53 CCND1 HRAS MAP2K1 TFG NCOA4
Lysine degradation	0,00081	2	WHSC1L1 SETD7 NSD1 ASH1L ALDH9A1 KMT2E
Proteasome	0,00081	2	PSMB8 PSMD2 PSME4 PSME2 PSMD13 PSMB2 PSMD1 PSMD7 POMP
Cell cycle	0,001	2	CCNB2 PCNA E2F1 CCNB1 CCND2 CDK1 CDK6 MCM7 TP53 CCND1 E2F5 SKP2 CDC20 CDC23 RBX1 RAD21

Figure 6. Cell miRNA related pathways after H_2O_2 exposure in ARPE-19 cells. Graphic representation of cellular pathways (Y) and $\log_{10}$ P-value (X), circle size represents the number of involved miRNAs up to 7 deregulated miRNAs. (**A**) KEGG pathways regulated and putative target genes (**B**).

A

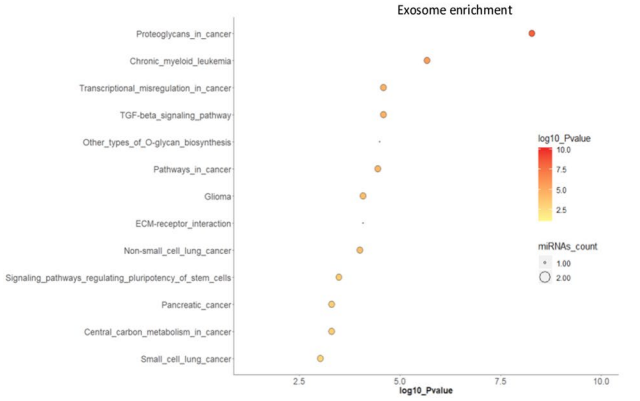

B

KEGG pathway	P_value	Number of miRNAs	Putative target genes
Proteoglycans in cancer	$5{,}23\times10^{-9}$	2	ACTB FZD5 ITGB1 EZR SOS2 SMAD2 CBL ARHGEF12 ROCK2 FZD6 IQGAP1 RAF1 IGF1R EGFR FZD3 PAK1 TP53 CTTN SLC9A1 DCN PLCG1 PIK3CD CCND1 AKT1 MYC FLNB PIK3CG PTPN11 RAC1 FZD1 ANK1 PDPK1 VIMP1 MTOR FGFR1 MAPK1 MDM2 RPS6KB1 CD44 PRKACB PPP1CB
Chronic myeloid leukemia	$2{,}14\times10^{-6}$	2	E2F1 TGFBR1 SOS2 CDK4 CBL E2F2 RUNX1 CTBP1 RAF1 CDKN1B TP53 PIK3CD CCND1 SMAD4 E2F3 AKT1 MYC NFKBIA PIK3CG PTPN11 MEDOM MAPK1 TGFBR2 MDM2
TGF-beta signaling pathway	$2{,}58\times10^{-5}$	2	TGFBR1 ID2 SMAD2 NODAL SMURF2 BMPR1B LEFTY1 ID4 ACVR2B ZFYVE16 DCN SMAD4 MYC RBL1 LTBP1 E2F4 MAPK1 SMAD1 TGFBR2 RPS6KB1
Transcriptional misregulation in cancer	$2{,}58\times10^{-5}$	2	CCNT2 NFKBIZ ID2 FUS ETV6 ELK4 RUNX1 AFF1 CCND2 CDKN1B MLLT3 IGF1R RUNX2 TP53 ATM MYC KLF3 PLAT FLT1 JMJD1C ETV1 BCL6 DOT1L PPARG KMT2A BCL2A1 EWSR1 SMAD1 TGFBR2 MDM2 TAF15
Other types of O-glycan biosynthesis	$3{,}19\times10^{-5}$	1	ST3GAL3 OGT POMT2 MFNG GXYLT1 B3GAT2 B4GALT1 POFUT1
Pathways in cancer	$3{,}55\times10^{-5}$	2	FZD5 E2F1 TGFBR1 ITGB1 SOS2 CDK4 LAMB1 SMAD2 CBL E2F2 CXCR4 STK4 GNAS LAMA5 RUNX1 TPR CTBP1 ARHGEF12 BAX ROCK2 FZD6 RAF1 CDKN1B TRAF4 PLD1 LPAR2 BRCA2 IGF1R EGFR APPL1 FZD3 VHL TP53 LAMC3 PLCG1 PIK3CD CCND1 SMAD4 MSH6 COL4A2 E2F3 AKT1 PGF F2R MYC NFKBIA KIT COL4A3 PIK3CG HSP90B1 RAC1 FGF18 FZD1 PPARG GNAQ PIAS2 CCNE1 MECOM CYCS MTOR FGFR1 MAPK1 TGFBR2 MDM2 PLCB4 PRKACB
ECM-receptor interaction	$8{,}31\times10^{-5}$	1	ITGB1 ITGB8 LAMB1 PAMA5 COL27A1 AGRN LAMC3 COL4A2 COL5A3 CD44
Glioma	$8{,}31\times10^{-5}$	2	E2F1 SOS2 CDK4 E2F2 RAF1 IGF1R EGFR TP53 PLCG1 PIK3CD CCND1 E2F3 AKT1 PIK3CG MTOR MAK1 MDM2
Non-small cell lung cancer	$9{,}84\times10^{-5}$	2	E2F1 SOS2 CDK4 E2F2 STK4 RAF1 EGFR TP53 PLCG1 PIK3CD CCND1 E2F3 AKT1 PIK3CG PDPK1 MAPK1
Signaling pathways regulating pluripotency of stem cells	0,0003	2	JARID2 FZD5 ID2 SMAD2 NODAL RBST BMPR1B TBX3 FZD6 RAF1 IGF1R ZFHX3 ID4 FZD3 ACVR2B RIF1 PIK3CD JAK2 SMAD4 AKT1 MYC SKIL PIK3CG FZD1 ISL1 FGFR1 SOX2 MAPK1 SMAD1
Pancreatic cancer	0,0005	2	E2F1 TGFBR1 CDK4 SMAD2 E2F2 RAF1 PLD1 BRCA2 EGFR TP53 PIK3CD CCND1 SMAD4 E2F3 AKT1 PIK3CG RAC1 MAPK1 TGFBR2
Central carbon metabolism in cancer	0,0005	2	PKM RAF1 EGFR SLC7A5 SLC16A3 G6PD TP53 PIK3CD AKT1 MYC KIT PIK3CG IDH1 MTOR FGFR1 MAPK1 SLC1A5
Small cell lung cancer	0,0010	2	E2F1 ITGB1 CDK4 LAMB1 E2F2 LAMA5 CDKN1B TRAF4 TP53 LAMC3 PIK3CD CCND1 COL4A2 E2F3 AKT1 MYC NFKBIA COL4A3 PIK3CG PIAS2 CCNE1 CYCS

Figure 7. sEVmiRNA related pathways after H_2O_2 exposure in ARPE-19 cells (**A**) Graphic representation of cell pathways (Y) and $\log_{10}$ P-value (X), circle size represents the number of involved miRNAs up to 2 deregulated miRNAs. (**A**) KEGG pathways regulated and putative target genes (**B**).

stress-related ones[23–26]. On this line, the use of RPE cell cultures, as ARPE-19 under oxidative challenges (eg. H_2O_2, rotenone or EtOH), results useful to study the RPE response to oxidative stimuli[27–29].

As mentioned earlier, 600 µM was the highest H_2O_2 concentration used which increased ROS levels without generating early apoptosis (800 µM H_2O_2 exposure significantly increased early apoptosis). Other authors have used different H_2O_2 ranges (200-600 µM) and some differences can be found in terms of cell viability (XTT or MTT), apoptosis and ROS production[7,27,30]. Plausibly, the differences on time exposure (12–24 h) or cell confluence level could explain these discrepancies.

Fitting with previous data, pro-oxidant challenge resulted on significant high sEVs release from ARPE-19 cells. It is well documented that EtOH or high glucose conditions resulted in the same response increasing sEVs release from ARPE-19 cells[28,31].

Extracellular or circulating miRNAs can be included on sEVs, associated to lipoproteins or proteins[13]. In this respect, we have just focused on miRNAs contained as sEVs cargo (sEV miRNA). In spite of the fact that in sEVs only 218 out of 384 miRNAs could be detected, only two sEV miRNAs were significantly high in control released sEVs than in sEVs from treated cells. The hsa-miR-302a and hsa-miR-122 have already been seen in sEVs confirming our results[32–35].

miRNA	Reference
hsa-miR-139-3p	Szemraj *et al.* and Ertekin *et al.*[17,52]
hsa-miR-192	Grassmann *et al.* and Ertekin *et al.*[24,52,53]
hsa-let-7c	Ren *et al.* and Szemraj *et al.*[17,19]
hsa-miR-18b	Ren *et al.* and Wang *et al.*[19,54]
hsa-miR-183	Karali *et al.*, Loscher *et al.* and Xiang *et al.*[55–57]
hsa-miR-23a	Li *et al.*, Lin *et al.*, Romano *et al.*, Szemraj *et al.* and Zhou *et al.*[7,16,17,47,58]
hsa-miR-27a	Ren *et al.*; Romano *et al.*; Szemraj *et al.*[16,17,19]
hsa-miR-25	Ren *et al.* and Zhang *et al.*[19,59]
hsa-miR-106a	Ertekin *et al.*[52]
hsa-let-7a	Ertekin *et al.* and SanGiovanni *et al.*[52,60]
hsa-miR-27b	Ertekin *et al.* and Howell *et al.*[30,52]
hsa-miR-518d-3p	Dinç *et al.*[27]
hsa-miR-92a	Dinç *et al.*, Howell *et al.*, Desjarlais *et al.* and Walz *et al.*[27,30,61,62]
hsa-miR-361-5p	Grassmann *et al.* and Szemraj *et al.*[17,24]
hsa-miR-335	Ertekin *et al.* and Grassmann *et al.*[24,52]
hsa-miR-30c	Ren *et al.*[19]
hsa-miR-28-5p	Ren *et al.*[19]
hsa-miR-29a	Ertekin *et al.*, Howell *et al.*, Walz *et al.*, Zhang *et al.* and Zhang *et al.* (2)[30,52,62–64]
hsa-miR-205	Ménard *et al.*[4]
hsa-miR-17	Ertekin *et al.*, Barber *et al.* and Tian *et al.*[5,18,52]
hsa-miR-324-5p	Ertekin *et al.*[52]
hsa-miR-302c	Howell *et al.*[30]
hsa-miR-30b	Dinç *et al.*, Romano *et al.*, Mazzeo *et al.* and Haque *et al.*[16,27,65,66]
hsa-miR-28-3p	Howell *et al.*[30]

Table 2. Relevant miRNAs identified on eye disorders.

When comparing the two sEV miRNAs, hsa-miR-302a and hsa-miR-122, to those miRNAs on ARPE-19 cells (Cell miRNA), no matches could be found. Surprisingly, the sEV miRNA hsa-miR-302a and the Cell miRNA hsa-miR-302c belong to the miR 302/367 *La-related protein 7* (*LARP7*) intragenic cluster. This includes hsa-miR-367, hsa-miR-302d, hsa-miR-302a, hsa-miR-302c, and hsa-miR-302b. This cluster is involved in several processes coordinating proliferation, differentiation, pluripotency maintenance, and cell reprogramming[36]. Moreover, the cluster, regulates TGF pathway, PI3K–AKT and BMP cell signaling[37–39]. Additionally, hsa-miR-302a acts as a tumor suppressor[40] and repressor of cell division, and more concretely, VEGFA is one of the direct targets for this miRNA[41]. In addition, hsa-miR-122 has been related to VEGFC[42]. Interestingly, low hsa-miR-302a/hsa-miR-122 expression levels are inversely related to VEGF levels in hepatocellular carcinoma, promoting vascular changes[43,44]. In addition, miR-122 seems to have a role against oxidative stress, since the use of pre-miR-122 protects from H_2O_2 induced oxidative stress[45], targeting the mitochondrial ribosomal protein S11[46].

Recent data from other groups indicate how diverse oxidative insults -EtOH or high glucose, and now H_2O_2 - lead to increased sEVs release from ARPE-19 cells[28,31]. Furthermore, those oxidative-induced sEVs were capable of promoting neovascular processes in endothelial cell cultures, whereas control-released sEVs inhibited this phenomenon[28,31]. In view of these findings, we hypothesize that sEVs hsa-miR-122 and hsa-miR-302a decreased levels could play a role on angiogenesis involving oxidative stress related pathways.

Several reports on AMD or experimental AMD, have reported significant changes on miRNAs (see Table 2). Among them, hsa-miR-23a is present in five reports[7,16,17,42,47]. This miRNA seems to be downregulated in both AMD patients and H_2O_2-treated ARPE-19 cells. In fact, H_2O_2 induced-apoptotic cell death is significantly observed in ARPE-19 cells after hsa-miR-23a inhibition[7]. Fitting with this, we found significant expression differences on hsa-miR-23a after H_2O_2 exposure (FC = 0.79). Table 2 summarizes those Cell miRNAs matching with previous reports on AMD or AMD experimental models. Besides, there are reports that locate the sEVS-miRNAs in eye tissue. MiR-302 expression was observed already in RPE cells by Li and collaborators, playing an important role in the RPE differentiation[48]. Other authors observed a miR-122 differential expression on canine retinas[49], in aqueous humor[50] and are related in fact with diabetic retinopathy[51]. In agreement with others, up/down regulated miRNAs are related to several and different cell signaling pathways. After seeing the results in both sEV miRNA and Cell miRNAs related pathways, cancer related pathways are commonly involved in many of the deregulated miRNAs. More research must be performed on these generic pathways to determine the concrete role of these cell signaling routes.

As a conclusion, H_2O_2 significantly increased sEVs release from ARPE-19 cells compared to control cells. Paradoxically, the miRNA sEVs cargo (hsa-miR-302a and hsa-miR-122) resulted in significantly lower in H_2O_2-induced sEVs compared to control. Since hsa-miR-302a and hsa-miR-122 regulates vasculogenic targets, these results support those on ARPE-19 cells indicating that oxidative-induced sEVs promote angiogenesis[28,31].

Material and Methods

Cell culture. Arising retinal pigment epithelium (ARPE-19) human cell line was obtained from American Type Culture Collection (ATCC, Barcelona, Spain) at passage 19. ARPE-19 cells were cultured in Dulbecco's modified Eagle's DMEM/F12 (Invitrogen, Carlsbad, CA, USA), as previously described[21]. Cells were used until passage 30. Cells were cultured to 80–90% confluence at a starting density of 1×10^6 cells/cm^2 in different plates depending on the technique. After 2 days, the cells were treated for 24 h with 600 µM H_2O_2 (Scharlau, Senmenat, Spain), using filtered media with 1% of Fetal Bovine Serum, exosome-depleted (FBS; Thermo Fisher Scientific, Gibco, USA). Cells and supernatant were collected and preserved for future experiments.

Determination of intracellular ROS. Intracellular ROS levels were measured using dihydroethidium, (DHE; Thermo Fisher Scientific, Waltham, MA, USA), which is a superoxide indicator. This molecule has a blue fluorescence, but, when oxidized to ethidium, it stains DNA in red. ARPE-19 cells were seeded at 6×10^3 cells/well in a 96 well plate. Cells were rinsed with PBS (phosphate-buffered saline) twice and incubated with 5 µM of DHE during 30 min at 37 °C and 5% CO_2. ROS levels were measured by a fluorescence multiplate reader (Victor X5; Perkin Elmer) excited at 518 nm and read at 605 nm.

Apoptosis detection. Number of dead cells by apoptosis or necrosis was measured by flow cytometry using the FITC Annexin V Apoptosis detection Kit (Immunostep, Salamanca, Spain) that can discriminate live cells from those in early apoptosis, late apoptosis, or necrosis. A total of 10,000 cells per condition were analysed using the FACS Verse (Beccton Dikinson, New Jersey, USA). Four populations are detected: unmarked Annexin (−)/Propidium Iodide (−) are live cells; double marked Annexin (+)/Propidium Iodide (+) represent apoptotic cells; simple marked Annexin (+)/Propidium Iodide (−) are early apoptotic cells; and simple marked Annexin (−)/Propidium Iodide (+) are necrotic cells.

sEVs isolation and size distribution. sEVs isolation was performed by successive ultracentrifugation as previously reported[21]. The sEVs pellet was stored at 4 °C until further processing in PBS solution. For microarray assay, sEVs were isolated using ExoQuick-TC (Systems Biosciences, Mountain View, CA, USA) following the manufacturer's instructions. sEVs identity was confirmed by the nanoparticle tracking system NanoSight NS300 following manufacturer's protocols (Malvern Instruments, Malvern, UK).

Electron microscopy. sEVs pellets were resuspended in PBS and ultracentrifuged at 120.000 × g for 70 min at 4 °C. After that, approximately 10 µg of the samples were resuspended in PBS on parafilm. The sample was fixed by depositing a drop of 2% Paraformaldehyde on the parafilm and placing the grid (Mesh with Formvar) on top of the drop. Negative staining was performed with 2% uranyl acetate. Photomicrographs were obtained using the transmission electron microscope FEI Tecnai G2 Spirit (FEI Europe, Eindhoven, Netherlands) using a digital camera Morada (Olympus Soft Image Solutions GmbH, Münster, Germany). EVs were identified under the microscope solely based on size and morphology.

RNA isolation and miRNA expression analysis. To perform microarray analysis, ARPE-19 cells from 4 separate cultures were exposed to control and H_2O_2 600 µM treatment for 24 h. Total RNA was extracted using SeraMir Kit (System Biosciences, Mountain View, CA, USA) according to manufacturer's instructions. Therefore, four microarrays were performed for each condition: control, ARPE-19 cells exposed to H_2O_2 600 µM, sEVs released by control cells and sEVs released by ARPE-19 cells exposed to H_2O_2 600 µM.

Total RNA quantity and quality (260/280 absorbance ratio) were assessed using NanoDrop 2000 (Thermo Fisher Scientific, Waltham, MA, USA). Total RNA was reversely transcribed (cDNA synthesis) using PeqSTAR 96 Universal Gradient (PeqLAb, Erlangen, Germany) under the following conditions: 60 °C/5 min, RT/2 min, 42 °C/30 min, 95 °C/10 min and 15 °C/hold. Real-time quantitative PCR (qPCR) was performed using 384 well SeraMir Profiler using RT-PCR QuantStudio™ 3 y 4 system (Thermo Fisher Scientific, Waltham, MA, USA) with the appropriate temperature cycles 50 °C/2 min, 95 °C/10 min, 40 ciclos; 95 °C/15 s, 6 °C/1 min. The miRNA expression values were calculated using three endogenous controls: RNU43, RNU1Q and RNU6. The expression was calculated according to the $2^{-\Delta\Delta Ct}$ method.

Array analysis. We analyzed miRNA expression differences between ARPE-19 control cells and ARPE-19 treated with H_2O_2. Moreover, differences in miRNA expression between EVs released by ARPE-19 cells treated and EVs released by ARPE-19 control cells were also studied. Differences were analyzed using a t-test study from *genefilter* package from R Bioconductor. *P-values* were adjusted by the Benjamini-Hochberg method. MiRNAs that presented an adjusted p-value < 0.05 were considered statistically significant. Significantly modified miRNAs from different samples were represented in a hierarchical clustering heatmap representation. Heatmaps were performed using *heatmap.3* package from R Bioconductor.

Analysis of miRNA target genes. *In silico* analysis of the pathways in which the miRNAs regulated by H_2O_2 were involved using DIANA TOOLS mirPath v.3 algorithm (http://snf-515788.vm.okeanos.grnet.gr/). Moreover, we carry out an analyse of the putative miRNAs target using TargetScanHuman (http://www.targetscan.org/vert_72/).

Quantitative real-time PCR validation. Quantitative real time PCR (qRT-PCR) was used to validate the miRNA expression profile of the selected miRNAs in an independent sample set. The RNA was isolated from ARPE-19 cells by miRNeasy Mini Kit (Qiagen, Hilden, Germany) according to the manufacturer's instructions.

100–300 ng of RNA were retro transcribed using TaqMan MicroRNA Reverse Transcription Kit (Thermo Fisher Scientific, Waltham, MA, USA) using specific TaqMan RT primers and the thermocycler PeqSTAR 96 Universal Gradient (PeqLAB, Erlangen, Germany), the cycles used were 16 °C/30 min, 42 °C/30 min, 85 °C/5 min and 4 °C/infinity. Quantitative real time PCR was performed using TaqMan™ microRNA Assays (Thermo Fisher Scientific, Waltham, MA, USA) with TaqMan Gene Expression master Mix (Thermo Fisher Scientific, Waltham, MA, USA) and RT-PCR Roche 234 LighterCycler 480 with the appropriate temperature cycles (50 °C/2 min, 95 °C/10 min, 40 cycles: 95 °C/15 s and 60 °C/1 min). Normalisation was performed with RNU6B snoRNA and RNU43 snoRNA. Relative expression was calculated as $2^{-\Delta\Delta Ct}$.

Statistical analysis. The results of each experiment are presented as mean ± SEM. Statistical significance was determined using t-test and 2-way-ANOVA.

Data availability

The datasets generated during and/or analysed during the current study are available from the corresponding author on reasonable request.

Received: 12 March 2019; Accepted: 14 November 2019;
Published online: 29 November 2019

References

1. Kumar, S., Vijayan, M., Bhatti, J. S. & Reddy, P. H. MicroRNAs as Peripheral Biomarkers in Aging and Age-Related Diseases. *Prog. Mol. Biol. Transl. Sci.* **146**, 47–94 (2017).
2. Bhaskaran, M. & Mohan, M. MicroRNAs: history, biogenesis, and their evolving role in animal development and disease. *Vet. Pathol.* **51**, 759–774 (2014).
3. Elbay, A., Ercan, Ç., Akbaş, F., Bulut, H. & Ozdemir, H. Three new circulating microRNAs may be associated with wet age-related macular degeneration. *Scand. J. Clin. Lab. Invest.* **79**, 1–7 (2019).
4. Ménard, C. *et al*. MicroRNA signatures in vitreous humour and plasma of patients with exudative AMD. *Oncotarget* **7**, 19171–19184 (2016).
5. Tian, B. *et al*. miR-17-3p Exacerbates Oxidative Damage in Human Retinal Pigment Epithelial Cells. *PLoS One* **11**, e0160887 (2016).
6. Yoon, C. *et al*. Delivery of miR-155 to retinal pigment epithelial cells mediated by Burkitt's lymphoma exosomes. *Tumor Biol.* **37**, 313–321 (2016).
7. Lin, H. *et al*. Effect of miR-23 on Oxidant-Induced Injury in Human Retinal Pigment Epithelial. *Cells. Investig. Opthalmology Vis. Sci.* **52**, 6308 (2011).
8. He, J.-F., Du, Y., Jiang, B.-L. & He, J.-F. Increased microRNA-155 and decreased microRNA-146a may promote ocular inflammation and proliferation in Graves' ophthalmopathy. *Med. Sci. Monit.* **20**, 639–643 (2014).
9. Turturici, G., Tinnirello, R., Sconzo, G. & Geraci, F. Extracellular membrane vesicles as a mechanism of cell-to-cell communication: advantages and disadvantages. *Am. J. Physiol. Cell Physiol.* **306**, C621–C633 (2014).
10. Yang, X., Weng, Z., Mendrick, D. L. & Shi, Q. Circulating extracellular vesicles as a potential source of new biomarkers of drug-induced liver injury. *Toxicol. Lett.* **225**, 401–406 (2014).
11. Février, B. & Raposo, G. Exosomes: Endosomal-derived vesicles shipping extracellular messages. *Curr. Opin. Cell Biol.* **16**, 415–421 (2004).
12. Théry, C. *et al*. Minimal information for studies of extracellular vesicles 2018 (MISEV2018): a position statement of the International Society for Extracellular Vesicles and update of the MISEV2014 guidelines. *J. Extracell. vesicles* **7**, 1535750 (2018).
13. Creemers, E. E., Tijsen, A. J. & Pinto, Y. M. Circulating MicroRNAs. *Circ. Res.* **110**, 483–495 (2012).
14. Biasutto, L., Chiechi, A., Couch, R., Liotta, L. A. & Espina, V. Retinal pigment epithelium (RPE) exosomes contain signaling phosphoproteins affected by oxidative stress. *Exp. Cell Res.* **319**, 2113–2123 (2013).
15. Wang, S., Koster, K. M., He, Y. & Zhou, Q. miRNAs as potential therapeutic targets for age-related macular degeneration. *Future Med. Chem.* **4**, 277–287 (2012).
16. Romano, G. L. *et al*. Retinal and Circulating miRNAs in Age-Related Macular Degeneration: An *In vivo* Animal and Human Study. *Front. Pharmacol.* **8**, 168 (2017).
17. Szemraj, M. *et al*. Serum MicroRNAs as Potential Biomarkers of AMD. *Med. Sci. Monit.* **21**, 2734–2742 (2015).
18. Berber, P., Grassmann, F., Kiel, C. & Weber, B. H. F. An Eye on Age-Related Macular Degeneration: The Role of MicroRNAs in Disease Pathology. *Mol. Diagnosis Ther.* **21**, 31–43 (2017).
19. Ren, C. *et al*. Circulating miRNAs as potential biomarkers of age-related macular degeneration. *Cell. Physiol. Biochem.* **41**, 1413–1423 (2017).
20. Kim, J. M. *et al*. Responses of Types 1 and 2 Neovascularization in Age-Related Macular Degeneration to Anti-Vascular Endothelial Growth Factor Treatment: Optical Coherence Tomography Angiography Analysis. *Semin. Ophthalmol.* **34**, 168–176 (2019).
21. Strauss, O. The Retinal Pigment Epithelium in Visual Function. *Physiol. Rev.* **85**, 845–881 (2005).
22. Hernández-Zimbrón, L. F. *et al*. Age-Related Macular Degeneration: New Paradigms for Treatment and Management of AMD. *Oxid. Med. Cell. Longev.* **2018**, 8374647 (2018).
23. Shen, J. *et al*. MicroRNAs Regulate Ocular Neovascularization. *Mol. Ther.* **16**, 1208–1216 (2008).
24. Grassmann, F. *et al*. A circulating MicroRNA profile is associated with late- stage neovascular age-related macular degeneration. *PLoS One* **9**, 1–8 (2014).
25. Magenta, A., Greco, S., Gaetano, C. & Martelli, F. Oxidative Stress and MicroRNAs in Vascular Diseases. *Int. J. Mol. Sci.* **14**, 17319–17346 (2013).
26. Baker, J. R. *et al*. Oxidative stress dependent microRNA-34a activation via PI3Kα reduces the expression of sirtuin-1 and sirtuin-6 in epithelial cells. *Sci. Rep.* **6**, 35871 (2016).
27. Dinç, E., Ayaz, L. & Kurt, A. H. Effects of Bevacizumab, Ranibizumab, and Aflibercept on MicroRNA Expression in a Retinal Pigment Epithelium Cell Culture Model of Oxidative Stress. *J. Ocul. Pharmacol. Ther.* **34**, 1–8 (2018).
28. Atienzar-Aroca, S. *et al*. Oxidative stress in retinal pigment epithelium cells increases exosome secretion and promotes angiogenesis in endothelial cells. *J. Cell. Mol. Med.* **20**, 1457–1466 (2016).
29. Ayaz, L. & Dinç, E. Evaluation of microRNA responses in ARPE-19 cells against the oxidative stress. *Cutan. Ocul. Toxicol.* **37**, 121–126 (2018).
30. Howell, J. C. *et al*. Global microRNA expression profiling: curcumin (diferuloylmethane) alters oxidative stress-responsive microRNAs in human ARPE-19 cells. *Mol. Vis.* **19**, 544–560 (2013).
31. Maisto, R. *et al*. ARPE-19-derived VEGF-containing exosomes promote neovascularization in HUVEC: the role of the melanocortin receptor 5 has been built and requires approval. *Cell Cycle* **18**, 413–424 (2019).

32. Bukong, T. N., Momen-Heravi, F., Kodys, K., Bala, S. & Szabo, G. Exosomes from hepatitis C infected patients transmit HCV infection and contain replication competent viral RNA in complex with Ago2-miR122-HSP90. *PLoS Pathog.* **10**, e1004424 (2014).
33. Mittelbrunn, M. *et al*. Unidirectional transfer of microRNA-loaded exosomes from T cells to antigen-presenting cells. *Nat. Commun.* **2**, 282 (2011).
34. van Balkom, B. W. M., Eisele, A. S., Pegtel, D. M., Bervoets, S. & Verhaar, M. C. Quantitative and qualitative analysis of small RNAs in human endothelial cells and exosomes provides insights into localized RNA processing, degradation and sorting. *J. Extracell. vesicles* **4**, 26760 (2015).
35. Jiao, X. *et al*. Serum and exosomal miR-122 and miR-199a as a biomarker to predict therapeutic efficacy of hepatitis C patients. *J. Med. Virol.* **89**, 1597–1605 (2017).
36. Gao, Z., Zhu, X. & Dou, Y. The miR-302/367 cluster: a comprehensive update on its evolution and functions. *Open Biol.* **5**, 150138 (2015).
37. Kuo, C.-H., Deng, J. H., Deng, Q. & Ying, S.-Y. A novel role of miR-302/367 in reprogramming. *Biochem. Biophys. Res. Commun.* **417**, 11–16 (2012).
38. Barroso-del Jesus, A., Lucena-Aguilar, G. & Menendez, P. The miR-302-367 cluster as a potential stemness regulator in ESCs. *Cell Cycle* **8**, 394–398 (2009).
39. Lipchina, I., Studer, L. & Betel, D. The expanding role of miR-302–367 in pluripotency and reprogramming. *Cell Cycle* **11**, 1517–1523 (2012).
40. Chen, W., Zhuang, X., Qi, R. & Qiao, T. MiR-302a-5p suppresses cell proliferation and invasion in non-small cell lung carcinoma by targeting ITGA6. *Am. J. Transl. Res.* **11**, 4348–4357 (2019).
41. Qin, C. *et al*. MicroRNA-302a inhibits cell proliferation and invasion, and induces cell apoptosis in hepatocellular carcinoma by directly targeting VEGFA. *Mol. Med. Rep.* **16**, 6360–6367 (2017).
42. Li, C. *et al*. Chronic inflammation contributes to the development of hepatocellular carcinoma by decreasing miR-122 levels. *Oncotarget* **7**, 17021–17034 (2016).
43. Qin, C. *et al*. MicroRNA-302a inhibits cell proliferation and invasion, and induces cell apoptosis in hepatocellular carcinoma by directly targeting VEGFA. *Mol. Med. Rep.* **16**, 6360–6367 (2017).
44. Wang, Y. *et al*. MiR-122 targets VEGFC in bladder cancer to inhibit tumor growth and angiogenesis. *Am. J. Transl. Res.* **8**, 3056–3066 (2016).
45. Bai, J. *et al*. DNA Methylation of miR-122 Aggravates Oxidative Stress in Colitis Targeting SELENBP1 Partially by p65NF- κ B Signaling. *Oxid. Med. Cell. Longev.* **2019**, 1–14 (2019).
46. Song, L. *et al*. MicroRNA-122 is involved in oxidative stress in isoniazid-induced liver injury in mice. *Genet. Mol. Res.* **14**, 13258–13265 (2015).
47. Zhou, Q. *et al*. Regulation of angiogenesis and choroidal neovascularization by members of microRNA-23~27~24 clusters. *Proc. Natl. Acad. Sci. USA* **108**, 8287–8292 (2011).
48. Li, W.-B. *et al*. Development of Retinal Pigment Epithelium from Human Parthenogenetic Embryonic Stem Cells and MicroRNA Signature. *Investig. Opthalmology Vis. Sci.* **53**, 5334–5343 (2012).
49. Genini, S., Guziewicz, K. E., Beltran, W. A. & Aguirre, G. D. Altered miRNA expression in canine retinas during normal development and in models of retinal degeneration. *BMC Genomics* **15**, 172 (2014).
50. Drewry, M. D. *et al*. Differentially expressed microRNAs in the aqueous humor of patients with exfoliation glaucoma or primary open-angle glaucoma. *Hum. Mol. Genet.* **27**, 1263–1275 (2018).
51. Pastukh, N., Meerson, A., Kalish, D., Jabaly, H. & Blum, A. Serum miR-122 levels correlate with diabetic retinopathy. *Clin. Exp. Med.* **19**, 255–260 (2019).
52. Ertekin, S. *et al*. Evaluation of circulating miRNAs in wet age-related macular degeneration. *Mol. Vis.* **20**, 1057–1066 (2014).
53. Wu, J. *et al*. Protective effects of methane-rich saline on diabetic retinopathy via anti-inflammation in a streptozotocin-induced diabetic rat model. *Biochem. Biophys. Res. Commun.* **466**, 155–161 (2015).
54. Wang, H.-C. *et al*. Profiling the microRNA Expression in Human iPS and iPS-derived Retinal Pigment Epithelium. *Cancer Inform.* **13**, 25–35 (2014).
55. Karali, M. *et al*. High-resolution analysis of the human retina miRNome reveals isomiR variations and novel microRNAs. *Nucleic Acids Res.* **44**, 1525–1540 (2016).
56. Loscher, C. J. *et al*. Altered retinal microRNA expression profile in a mouse model of retinitis pigmentosa. *Genome Biol.* **8**, R248 (2007).
57. Xiang, L. *et al*. miR-183/96 plays a pivotal regulatory role in mouse photoreceptor maturation and maintenance. *Proc. Natl. Acad. Sci.* **114**, 6376–6381 (2017).
58. Li, Ddan *et al*. Inhibition of the oxidative stress-induced miR-23a protects the human retinal pigment epithelium (RPE) cells from apoptosis through the upregulation of glutaminase and glutamine uptake. *Mol. Biol. Rep.* **43**, 1079–1087 (2016).
59. Zhang, J. *et al*. miR-25 Mediates Retinal Degeneration Via Inhibiting ITGAV and PEDF in Rat. *Curr. Mol. Med.* **17**, 359–374 (2017).
60. SanGiovanni, J. P., SanGiovanni, P. M., Sapieha, P. & De Guire, V. miRNAs, single nucleotide polymorphisms (SNPs) and age-related macular degeneration (AMD). *Clin. Chem. Lab. Med.* **55**, 763–775 (2017).
61. Desjarlais, M. *et al*. MicroRNA expression profile in retina and choroid in oxygen-induced retinopathy model. *PLoS One* **14**, e0218282 (2019).
62. Walz, J. M. *et al*. Impact of angiogenic activation and inhibition on miRNA profiles of human retinal endothelial cells. *Exp. Eye Res.* **181**, 98–104 (2019).
63. Zhang, Y. *et al*. Regulation of Matrix Metalloproteinase-2 Secretion from Scleral Fibroblasts and Retinal Pigment Epithelial Cells by miR-29a. *Biomed. Res. Int.* **2017**, 1–7 (2017).
64. Zhang, Y. *et al*. miR-29a regulates the proliferation and differentiation of retinal progenitors by targeting Rbm8a. *Oncotarget* **8**, 31993–32008 (2017).
65. Mazzeo, A. *et al*. Functional analysis of miR-21-3p, miR-30b-5p and miR-150-5p shuttled by extracellular vesicles from diabetic subjects reveals their association with diabetic retinopathy. *Exp. Eye Res.* **184**, 56–63 (2019).
66. Haque, R. *et al*. MicroRNA-30b-Mediated Regulation of Catalase Expression in Human ARPE-19 Cells. *PLoS One* **7**, e42542 (2012).

Acknowledgements

The present project was supported by internal funds from Universidad Católica de Valencia San Vicente Mártir (2018-128-001), Centro de Investigación Traslacional San Alberto Magno de la UCV (2019-128-001), and Conselleria de Educación, Investigación, Cultura y Deporte; Generalitat Valenciana (PROMETEO/2016/094). Oltra M and Vidal-Gil L, PhD training program fellowship UCV (EDUCV-PRE-2016-005 and EDUCV-PRE-2015-006 Personal Investigador en Formación UCV, respectively).

Author contributions

M.O. Cell cultures and sEVs isolation, flow citometry, miRNA extraction and quantification, qPCR, validation. L.V.G. Cell cultures and sEVs isolation, electronic microscopy. R.M. Cell cultures and sEVs isolation. S.S.O. Statistical analysis. F.J.R. MS revision and interpretation of results. J.S.P. Corresponding author and discussion. J.M.B. supervision and MS writing.

Competing interests

The authors declare no competing interests.

Additional information

Correspondence and requests for materials should be addressed to J.S.-P.

Reprints and permissions information is available at www.nature.com/reprints.

Publisher's note Springer Nature remains neutral with regard to jurisdictional claims in published maps and institutional affiliations.